# ######## TECHNICAL DESIGN ASSIGNMENT: BAND-PASS FILTER AND PCB DESIGN

Aleksandre Meskhi

6 May 2025

UNIVERSITY OF SURREY ########@surrey.ac.uk

# Table of Contents

## 1. Introduction

Band-pass filters are essential electronic circuits that allow signals within a specific frequency range to “pass” through, while attenuating signals which are outside this range. Often used in telecommunications and audio applications, these types of filters isolate and clean up the received signal, removing low and high frequency noise and minimizing interference from adjacent frequency sources. This is accomplished by combining the properties of low and high pass filters into a single one. Multiple different designs of such filters exist, the choice between the use of which, depends on the application.

The following report presents the design and development steps of a band-pass filter commonly used in telecommunications and especially popular in audio applications - $2^{rd}$ order Butterworth Sallen-key Band-pass filter; Detailing its operation, analysis, and circuit layout, alongside relevant calculations, and design parameters necessary for manufacturing. Together with this, relevant steps taken for PCB and enclosure development are provided.

## 2. Design Requirements and background information

### 2.1 Audio filtering background Information

As mentioned, the band-pass design used in most circuits, directly relies on the application. For audio applications, filters are frequently integrated into systems like mixers, equalizers and crossover networks for specific band (range) isolation and noise suppression. In these setups, it is crucial to preserve the original amplitude of the audio signals present within the passband. To achieve this, the filter must have a flat passband response, meaning minimal gain variation should be present between various frequencies within the passband. Another key criterion for audio applications is the amount of attenuation (amplitude reduction) present at frequencies directly before or after the cutoff frequencies (minimum and maximum frequency thresholds). The property describing this behavior is known as the roll-off rate, which needs to be steep.

Due to these considerations, Sallen-key topology filters are often favored for use in audio devices. These filters have low component counts, only 2 resistors and 2 capacitors alongside a feedback operational amplifier, which minimizes potential error sources and parasitics. Together with this, the quality of filtering is least dependent on the op-amp’s performance, which allows for great component price cuts.

### 2.2 Key design requirements

The pass band of the filter designed in this document has cutoff frequencies of 200Hz and 4300Hz, significant in voice communications. Most telephone systems limit audio inputs to this range to focus on speech intelligibility [6]. The cutoff frequency of a filter represents a specific value for which the power carried by the input signal is halved on the output, causing the gain of said filter to be equal to $\frac{1}{\sqrt{2}} = 0{,}707\ (-3Db)$ at $f_c$.

The circuit will make use of Sallen-key LPF (Low pass filter) and HPF (high pass filter) filters cascaded to produce a BPF (band pass filter). The practical implementation of the circuit design consists of a PCB mounted on an enclosure with SMA (coaxial) connectors, purposed for mono (single channel) audio. Alongside the input and output connections, external power is required for operational amplifiers, for which an additional centre tap circuit design is required (further details in the later sections).

# 3. Circuit Design

## 3.1 Conceptual circuit diagram

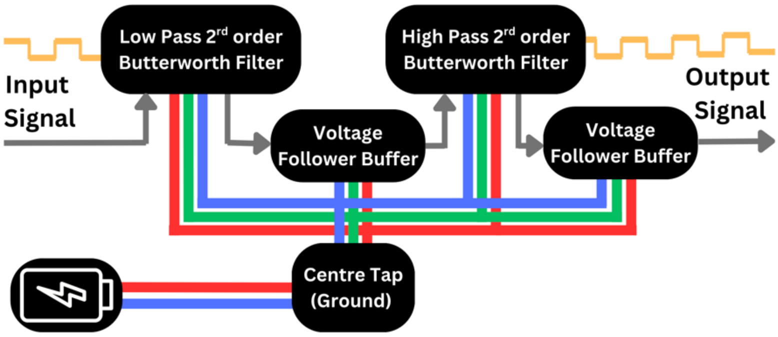


**Figure 1 – Operation block diagram of the band-pass filter [4]**

Figure 1 shows the operation block diagram of the band-pass filter used. As seen, the circuit can be subdivided into 3 main stages with 2 additional intermediate buffer stages. The input signal is first present on the LPF, which attenuates all components with frequencies greater than 4300Hz. The output of this filter is connected to a buffer, the purpose of which is to isolate the LPF from the rest of the circuit to eliminate loading effects (causing cutoff frequency changes and signal distortion). The output of the first buffer (left in figure 1) is connected to an HPF which removes all signal components with frequencies below 200Hz, the output of which is connected to the final buffer (right) to produce a stable output which will remain independent of the load connected.

As mentioned, operation amplifiers used in the filter design require external power. This must be provided in the form of a positive and a negative voltage reference, alongside a 0V ground. To achieve this, a centre tap circuit is used, the power rails of which can be seen to connect to all remaining stages.

## 3.2 Stage circuit schematics

### 3.2.1 Low Pass filter

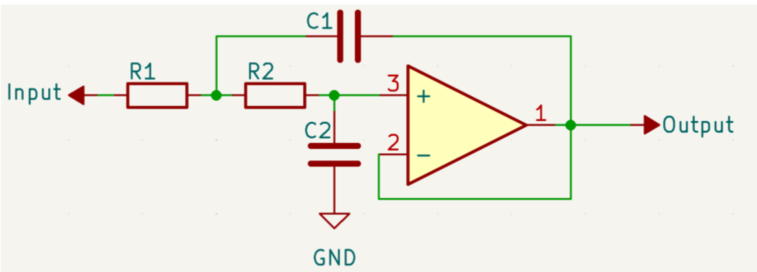


**Figure 2 – Low pass 2nd order Sallen-key Butterworth filter [2]**

Figure 2 shows the first operational stage of the BPF design, the low pass filter. As mentioned, this filter uses Sallen-key topology, utilizing only 2 resistors, 2 capacitors and a single op-amp. At low input frequencies, the capacitors C1 and C2 can be approximated to act as open connections, hence leaving the op-amp in a voltage follower configuration, and passing the input onto the output. On the other hand, at high frequencies, C2 can be approximated as a short, hence dissipating the signal through R1 and R2 to ground.

The cutoff frequency of the filter shown can be calculated by considering the impedances of the components used, alongside op-amp rules. Additionally, for ease of the calculations, resistors used are of equal value and the ratio $C_1/C_2$ is equal to 2. Using this, the following relations can be shown:

$$for\ \ R_1 = R_2\ \ \&\ \ C_2 = \frac{C_1}{2}, \qquad f_c = \frac{1}{2\pi\sqrt{R_1R_2C_1C_2}} = \frac{\sqrt{2}}{2\pi RC_1} \qquad [EQ.1]$$

By considering the E24 common resistor values, capacitors of 1nF and 2nF were chosen. For these, the resistance can be calculated to be $R = 26.163k\Omega \sim 26.1k\Omega$ (Closest E48 value). For these component values, the cutoff frequency was calculated to be $f_c = 4311.85Hz\ (0{,}275\%\ above)$.

As seen, the calculated cutoff frequency is highly accurate. Having said this, component tolerances might produce a larger error in this value. For $1nF \pm 1\%, 2nF \pm 1\%, 26.1k\Omega \pm 0.1\%$:

$$Tolerance = \pm\left(1 - \frac{1}{1.001\sqrt{1.01^2}}\right) = \pm 1.09\% \qquad \ggg \qquad f_c \in [4264Hz;\ 4359Hz]\ range$$

Overall, the calculations prove high accuracy of the LPF design which have been confirmed by simulations shown in later sections of this document.

### 3.2.2 High Pass filter

Figure 3 shows the second operational stage of the BPF design, the high pass filter. As mentioned, this filter uses Sallen-key topology, utilizing only 2 resistors, 2 capacitors and a single op-amp.

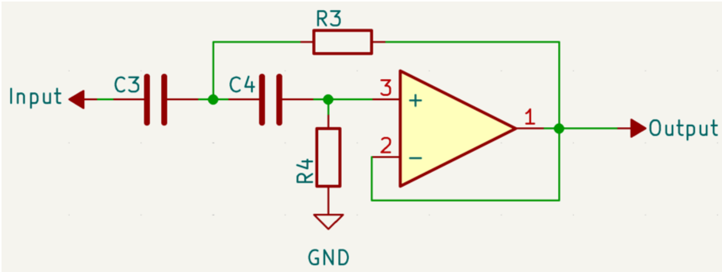


**Figure 3 – High pass 2nd order Sallen-key Butterworth filter [2]**

At low input frequencies, the capacitors C3 and C4 can be approximated to act as open connections, hence not allowing the input signal through. On the other hand, at high frequencies, C3 can be approximated as a short, hence passing the signal through R3 onto the output and since the inverting input is connected to the output of the op-amp, it tries to maintain the signal present on the non-inverting input, same as the initial input of the filter.

The cutoff frequency of the filter shown can be calculated by considering the impedances of the components used, alongside op-amp rules. The equations produced are almost identical to the LPF discussed in the previous section. Similarly, for ease of the calculations, capacitors used are of equal value and the ratio $R_3/R_4$ is equal to 2. Using this, the following relations can be shown:

$$for\ \ C_3 = C_4\ \ \&\ \ R_3 = \frac{R_4}{2}, \qquad f_c = \frac{1}{2\pi\sqrt{R_3R_4C_3C_4}} = \frac{\sqrt{2}}{2\pi CR_3} \quad [EQ.1]$$

By considering the E24 common resistor values, resistors of 120kΩ and 240kΩ were chosen. For these, the capacitance can be calculated to be $C = 4.689nF \sim 4.7nF$ (Closest E24 value). For these component values, the cutoff frequency was calculated to be $f_c = 199.54Hz\ (0{,}231\%\ below)$.

As seen, the calculated cutoff frequency is highly accurate. However, component tolerances may produce larger errors in this value. For $4.7nF \pm 1\%, 120k\Omega \pm 0.1\%, 240k\Omega \pm 0.1\%$ used:

$$Tolerance = \pm\left(1 - \frac{1}{1.01\sqrt{1.001^2}}\right) = \pm 1.09\% \qquad \ggg \qquad f_c \in [197Hz;\ 202Hz]\ range$$

Overall, the calculations prove high accuracy of the HPF design which have been confirmed by simulations shown in later sections of this document.

## 4. Centre Tap Circuit

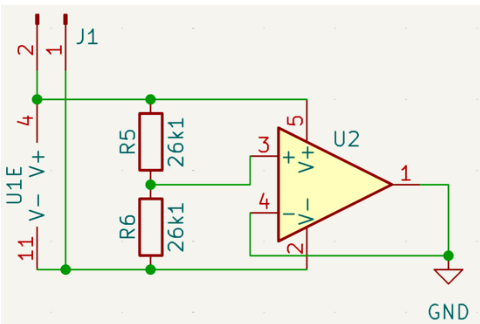


**Figure 4 – Centre Tap circuit [2]**

Figure 4 shows a centre-tap circuit, implemented to produce a virtual ground and symmetrical positive/negative voltage rails from a single DC input. As seen, two resistors of equal value (26,1kΩ) are used in a voltage divider configuration. The middle node of the divider will be at a voltage equal to half of that of the input voltage. This node is connected to an operational amplifier in a buffer (voltage follower) configuration, based on which the divider's midpoint voltage is maintained regardless of moderate load variations. The op-amp has a high input impedance, hence drawing negligible current from the divider, preserving the intended ±V reference. Its low output impedance allows it to supply or sink the necessary current to the load without letting the voltage change significantly. Under the assumption of a 5V input voltage ($\pm 2{,}5V\ rails$), the use of 26,1kΩ resistors will produce a current through them equal to: $I_{divider} = V_{in} \div (R_5 + R_6) \approx 0{,}1mA$. This value allows for a stable virtual ground production, while keeping the current consumption low. Additionally, using same value resistors as the ones used in the LPF (figure 2) will reduce the cost by allowing "bulk discount" use. Due to the low tolerance of the resistors (0,1%), the virtual ground will have a negligible error range of $\pm$2,5mV. Having said this, since the two resistors will be from the same batch, this error will be much smaller.

## 4.1 Complete BPF circuit design

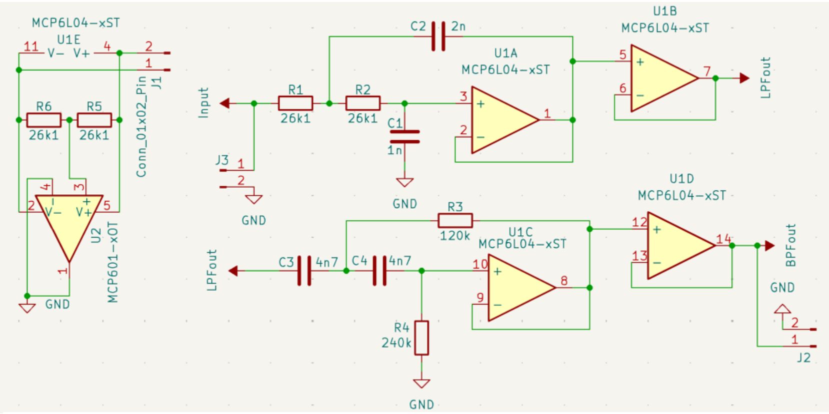


Figure 5 – Complete 2nd order Sallen-key Butterworth BPF circuit schematic [2]

Figure 4 shows the complete schematic of the BPF circuit. As mentioned, buffers are added between the LPF and HPF and before the output. A quad Op-amp IC has been used with four op-amps U1A-D, with its 2 power pins connected to an input socket. Virtual ground is created using a single op-amp IC (U2) in a centre tap circuit.

## 4.2 Circuit Simulation and final device operation specifications

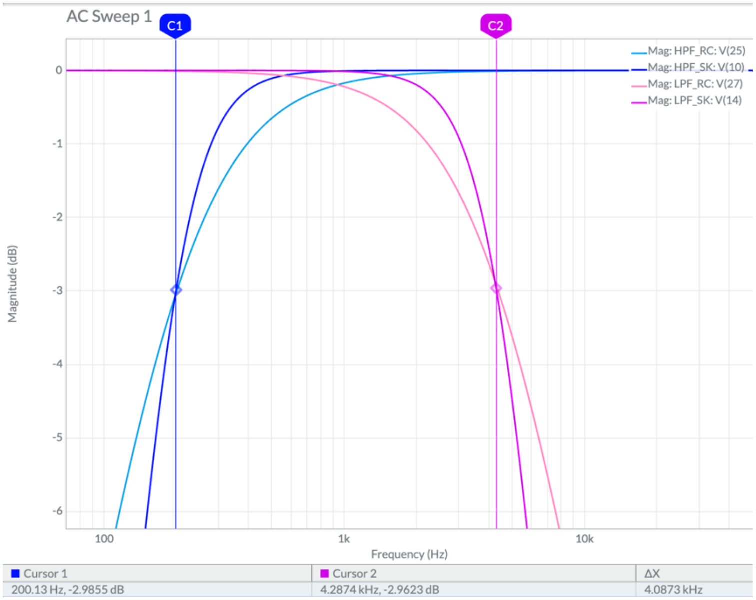


Figure 6 – Frequency response of the LPF and HPF filters [1]

A full circuit simulation was carried out for the proposed circuit design shown in figure 5. Initial testing confirmations involved checking the centre tap circuit current consumption (measured at 0,096mA as expected).

Before testing the two filters' joint operation, these were tested individually. Figure 6 shows the frequency response of the two Sallen-Key filters (LPF & HPF), alongside the frequency response of the simple RC LPF and HPF equivalents for operation quality comparison. The y axis is the gain of the filters in decibels, with the x-axis being the frequency (log scale).

The two cursors (C1 and C2) point to the -3Db point (significance explained in section 2.2). As seen under the graph, these two cursors point to $\sim 200Hz$ & $\sim 4.3kHz$. Hence the cutoff frequencies have been confirmed for the component choices. Comparing the two different filter designs, the transition band (just before cutoff frequencies) is narrower for the Sallen-Key filters. This means input signals at frequencies close to the cutoffs will not be attenuated, separating the passband from the stopband more precisely. Due to the proposed filter being 2$^{nd}$ order, their roll-off rates are double of the simple RC filters (40dB/dec instead of 20). Due to the passband being quite narrow (1,33 decades), simple RC filters can be seen to produce a passband which is not sufficiently flat and does not reach a 0 gain. This will cause attenuation of the input even for middle frequencies. Looking at the curves of the Sallen-key filters, approximately 30% of the bandpass can be seen to have a 0 gain. This is sufficiently flat for audio manipulation purposes.

To further confirm the operation of the band-pass filter, figure 7 shows the frequency response of the overall circuit's (as shown in figure 5) output. Together with this, the frequency response of the simple RC band-pass filter, with a buffer connected between the LPF and HPF, is shown.

As seen from the graph, the two cursors pointing to the -3Db gain, once again confirm the correct cutoff frequencies. Together with the gain, the phase curves for both filters are shown using dashed lines. The phase response of the Sallen-Key BPF can be seen to be double of the simple RC. This introduces greater phase shifts near the cutoff frequency which cause some phase distortion. However, the trade-off is acceptable in most telephony applications, where intelligibility is prioritized over prefect phase linearity.

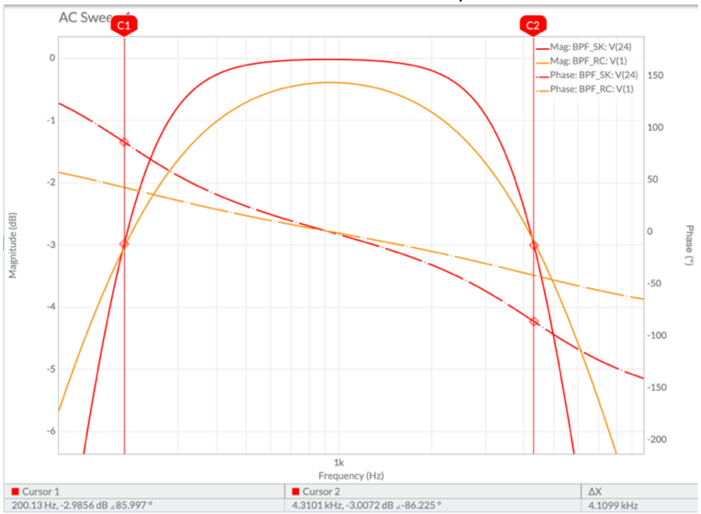

**Figure 7 – frequency response of the BPF [1]**

Overall, both figures 6 and 7 confirm that the component value choices are appropriate and that the proposed BPF operates as intended. The measured cutoff frequencies of the filter align meet the proposed specifications, and the phase response of $\pm 90°$ for the two $f_c s$ has also been confirmed. The roll-off rate of 40Db per decade can be seen, alongside a flat and stable passband, indicating reliable filter performance.

## 4.3 Final Operation specifications

| | |
|---|---|
| **Power input voltage** | **2,7 V – 6 V single supply (MCP601 requirement)** |
| **Minimal Current consumption** | $\boldsymbol{at\ 5V\ input \sim 0,7mA\ \ (> 230uA + 4 * 85uA + 0,1mA\ )}$ |
| **Minimal Power consumption** | $\boldsymbol{at\ 5V\ input \sim 3,5mW}$ |
| **Input signal maximum amplitude** | **2,95 V (50mV output swing)** |
| **Filter Type** | **2nd order Sallen-Key Butterworth Bandpass filter** |
| **Lower Cutoff frequency** | $\boldsymbol{f_{cLower} \in [197Hz;\ 202Hz]}$ |
| **Upper Cutoff frequency** | $\boldsymbol{f_{cUpper} \in [4264Hz;\ 4359Hz]}$ |
| **Centre Frequency** | $\boldsymbol{f_{centre} \in [917Hz;\ 939Hz]}$ |
| **Centre Frequency gain** | **0 Db** |
| **Roll-off Rate** | **40 Db/Decade** |

**Table 1 – Operation Specifications of the proposed BPF circuit, based on real component tolerances/specifications**

Table 1 shows the final operation specifications of the designed bandpass filter. The first three rows of the table describe the input power limitations and requirements. Overall, the filter requires very little power of 3,5mW to operate, when provided by a DC source of 5V. This value was calculated based on the quiescent currents of the ICs. Importantly, the source must not be internally grounded with respect to the input signal. For internally grounded PSUs, two of them can be used with each producing $\pm$2,5V.

The input signal amplitude must be considered for correct operation of the device. Since both ICs used are rail-to-rail op-amps, the output swing of these is not large. However, the amplitude must remain under $\frac{V_{DC}}{2} - 50mV$. The lower and upper cutoff frequencies of this filter are presented in ranges, influenced by the tolerances of the components used. The centre frequency input signals will have a gain of 0Db as required, with the gain roll-off rate of 40Db/decade for inputs outside the passband. Overall, the designed circuit meets all the specifications outlined in section 2, with enough flexibility with regards to the input DC power voltages and input signal amplitudes.

# 5. PCB design and component choices

## 5.1 Components and PCB property overview

The PCB design of this circuit will be implemented using SMD components, since the op-amp ICs mentioned are available in low-power SMD variants. Together with this, the smaller scale of the components will allow for shorter traces – improving electrical performance, reduced cost, and the overall compact design of the device.

To allow for manufacturing compatibility, the following design was developed according to JLCPCB's manufacturing capabilities (https://jlcpcb.com/capabilities/pcb-capabilities).

The resistors and capacitors used in this filter design are 1608 metric (0603 imperial) surface-mount components. The connectors used for input and output signals are SMA Jack edge mount coaxial male connectors. For providing DC power to the circuit, a JST EH series horizontal THT connector was used. The specific IC dimensions can be found by following the product links in the "Pricing and component list" section of this report.

## 5.2 Design process and decisions

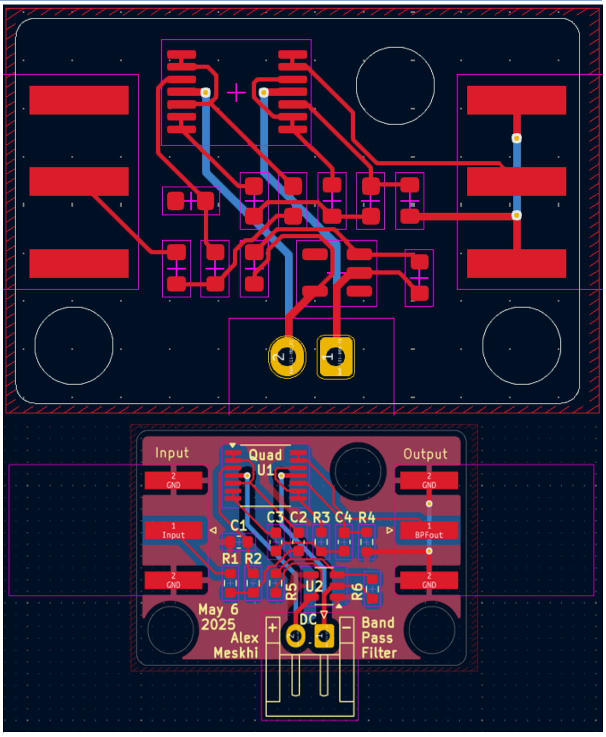


**Figure 8 – PCB design of the proposed BPF circuit [2]**

The initial design steps included drawing the schematic presented in figure 5 in KiCad. Following this, footprints of each component were assigned and the PCB rules were imported from the JLCPCB manufacturing capabilities. Individual components were grouped based on operational stages, after which their positions were varied until the trace crossover complexity of the design was reduced to its minimum. Since the signal connectors make use of both sides of the board, and the DC input connector is a Through-hole component, the PCB design was chosen to have 2-layers.

Following component placement optimization, trace widths were chosen. The previous sections outlined the minimal current consumption of the filter at 0,7mA. To remain on the safe side, the multiple traces coming directly out of the DC power input were chosen to have a track width equal to that of the MCP6L04T IC's power input pins, which is equal to 0,4mm or 16mil. According to IPC-2221 guidelines [7], a 0,4mm trace on a 1oz (35um) copper layer (JLCPCB value) can safely carry up to 1A of current with a 10°C temperature rise. Hence, these traces are sufficiently wide for the design. The rest of the connections are utilized using a 0,2mm of 8mil wide tracks. This value can handle current up to 0,7A with a 10°C temperature rise, which is sufficiently large to accommodate for common input signals, whilst allowing for escape routing (making traces between the SMD component pads), reducing the number of vias needed.

To ensure reliable grounding and signal integrity, full copper ground pours were added on both the front and back layers. Clearance values of 0,2mm were enforced for this net based on JLCPCB minimum spacing. Further realignment was required to to allow for enough space for at least 2 thermal relief pads per ground connection. The routing process mostly involved creating short traces, however some of the routes were more difficult to access than others, requiring longer tracks. Following layout completion, DRC (Design rules check) was ran, confirming that the design adheres to the required manufacturing and electrical clearance standards.

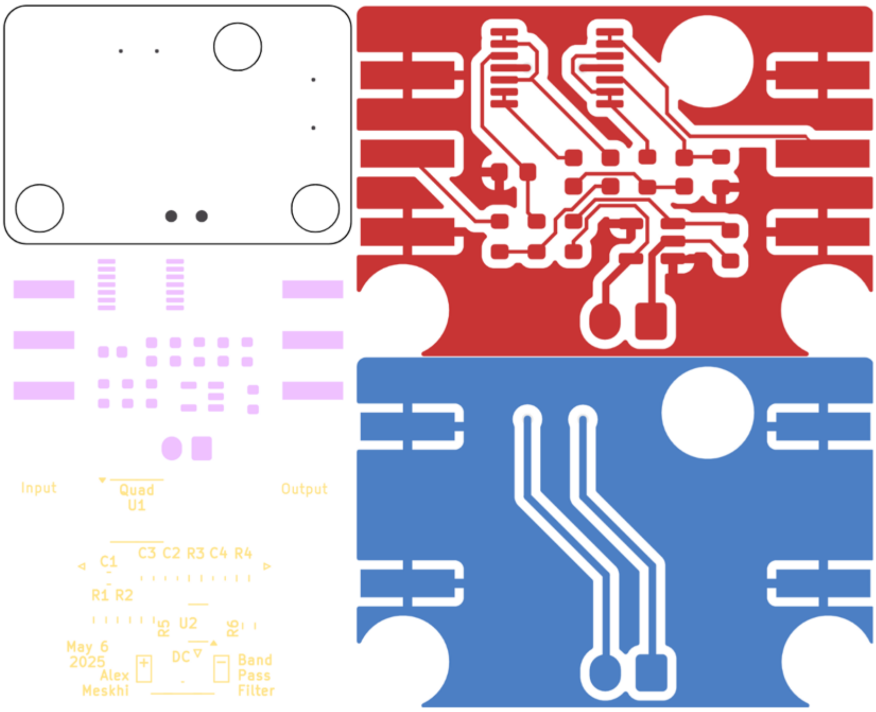


**Figure 9 – BPF filter PCB design Front and Back copper layers, alongside the edge cuts & drill holes, component masks and the front silkscreen. [2] [4]**

Most of the front and back layer tracks (red and blue in figure 8) cross perpendicularly, reducing interplane parasitic capacitance. The design makes use of only 4 vias, two of which are used to connect the input DC power to the quad op-amp IC. This connection would be much longer and unreliable without the use of vias. The other two, are used to connect the front and back ground fill zones, to ground all 4 ground pins of the signal connectors for noise reduction.

## 5.3 Full PCB Design and layout

Figure 10 below, shows the 3D model of the final PCB design with the components placed on the left side, and with the components disconnected and the front silkscreen hidden on the right side. Both front and back layers can be clearly viewed, with all the tracks and the fill zone.

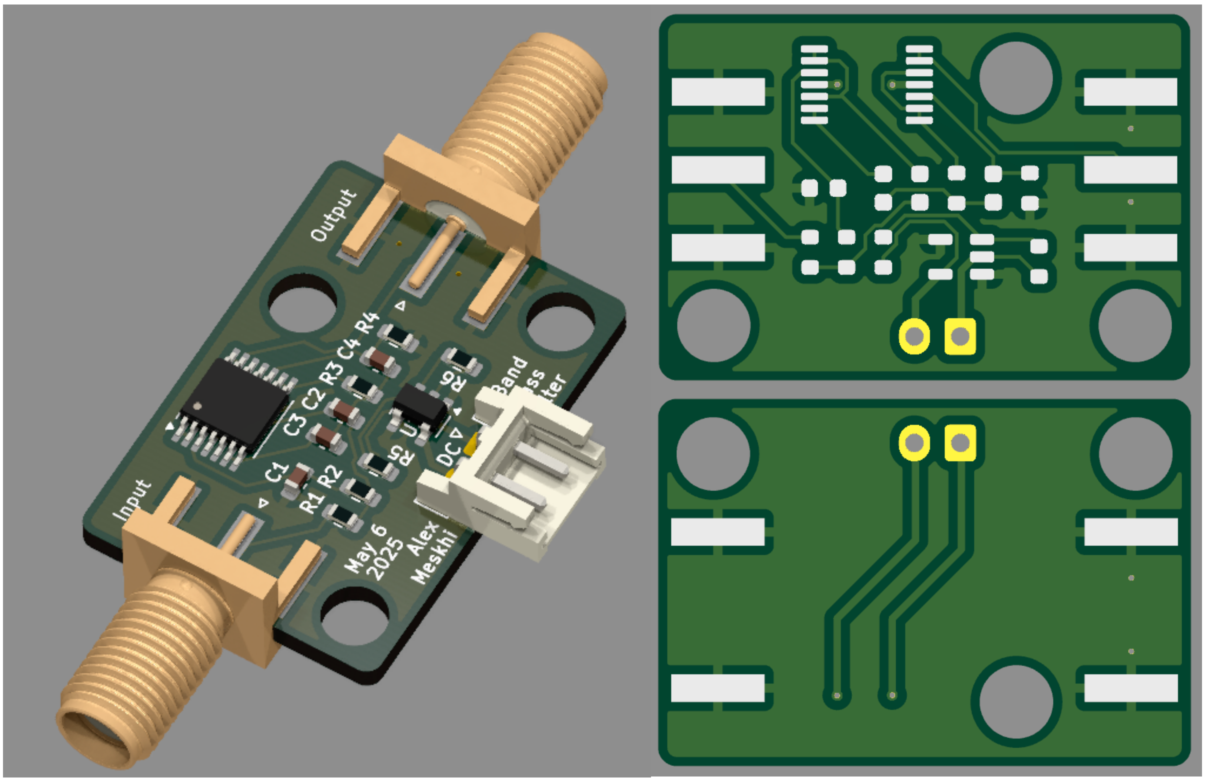


**Figure 10 – BPF PCB 3D model with the components placed (left) and with the components removed and front silkscreen not visible viewed from front and back (right). [2]**

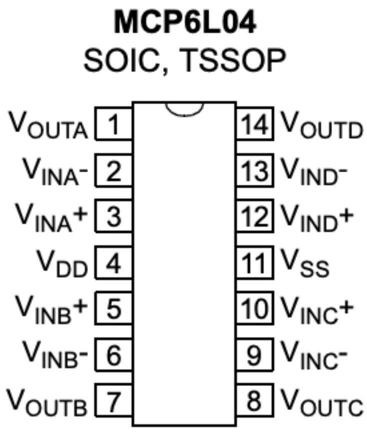


**Figure 11 – pinout of the MCP6L04 Quad op-amp IC [8]**

The final PCB layout demonstrates a compact and functionally segmented design. The board comprises a two-layer configuration, with all the signal traces and the majority of power traces distributed on the front layer. The layout adheres to logical groupings of components based on functional stages. The components used for the LPF are strategically placed on the left-hand side of the quad op-amp IC, the pinout of which is shown in figure 11. Pins 1-3 & 5-7 are used as the two op-amps needed for this stage, allowing for short traces to the input connector and the IC. The HPF is present on the right-hand side, utilizing the remaining two op-amps, while providing a clear path to the output connector. The second IC, MCP601T, is placed above the DC input connector, alongside the two resistors used in the centre tap circuit.

The SMD components are aligned and spaced for easy pick-and-place assembly, either by hand or automated. Three mounting holes are provided to allow for secure positioning within the enclosure, while utilizing the empty space on the PCB. The Silkscreen provides labels for all the components for ease of assembly, alongside relevant metadata; product purpose, date, and the designer details.

# 6. Enclosure

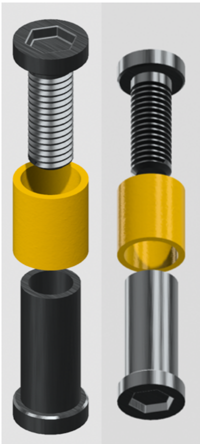

**Figure 12 – Barrel nut and bolt with spacer [3]**

## 6.1 Materials and key considerations

Multiple additional materials are required for the assembly of an enclosure. Based on the compact design of the PCB, 3D printing the enclosure would likely be the easiest and cheapest solution. PETG (polyethylene terephthalate glycol) material can be used to produce a strong and impact resistant enclosure. This material would also allow for precise printing due to its great layer adhesion. Due to the size of the enclosure and the bolts (M3 – 3mm diameter), thread tapping the material would not be an ideal choice, due to low torque resistance of the setup, alongside deformations over time. This is the primary reason a decision of using barrel nut and bolt pair was made, to securely mount the PCB onto the enclosure. A 3D models of the barrel nut and the bolt, alongside a spacer used, are presented in figure 12.

## 6.2 Enclosure 3D model

Figure 13 shows a 3D model of the enclosure used for the designed BPF. This enclosure measures 22mm×33,5mm×17,5mm. As seen, the “box” shape is built up of two individual sections, threaded to reduce wobble between them. Three areas, directly below the mounting holes on the PCB are raised to allow flush positioning. The top and bottom sides have circular cutouts for connector positioning. One side of the enclosure is cut to allow the DC power port access. As previously mentioned, the PCB will be mounted using barrel nut and bolt pair, which will at the same time connect the two sections of the enclosure together.

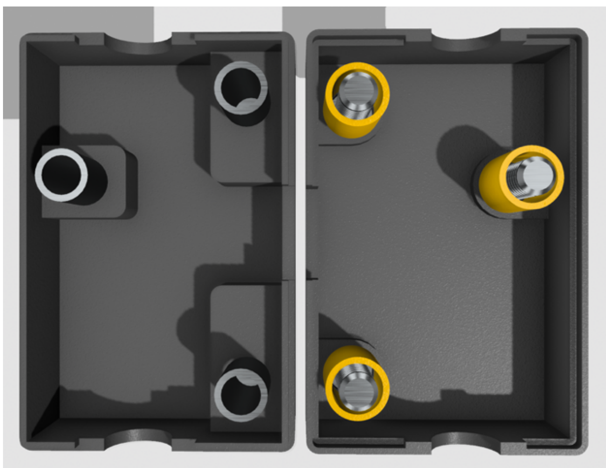

**Figure 13 – Device Enclosure without the PCB [3]**

# 7. 3D model and dimensions of the final product

## 7.1 3D model of the final product

Figure 14 shows a 3D-rendered model of the band pass filter fully assembled on a PCB, alongside its enclosure and mounting bolts. On the left-hand side, the exploded view of this device can be seen with the back casing (bottom) housing the barrel nuts, which also go through the PCB's mounting holes. The PCB is secured between the two halves of the enclosure using yellow-colored (3D printed, insulator material) spacers, through which the bolts pass and thread into the barrel nuts below. This, not only mounts the PCB, but fastens the top and bottom case shells as well. As seen, the sides of both halves are equipped with cutouts to accommodate for the SMA connectors (input/output) as well as the DC power input connector.

On the right-hand side, figure 14 shows the assembled device with the top half (top enclosure, bolts, and spacers) removed, together with the device viewed from the bottom with the bottom half (bottom enclosure and barrel nuts) removed. All the connectors on the PCB can be seen to sit flush with either side of the enclosure, showing the reliability and mechanical integrity of the design. None of the traces connect to the conductive bolts, or the spacers. The back layer of the PCB sits flush on the "extended" sections of the bottom half of the enclosure, but even so, the traces have been ensured to route around these sections.

Overall, this design allows for a quick and easy installation, requiring direct SMA connection for both the input and the output signals, maintaining the direction of the signal flow (connectors sit on the same line). The DC input is perpendicular to the connectors allowing for easy power connection without any interference with the signal cables.

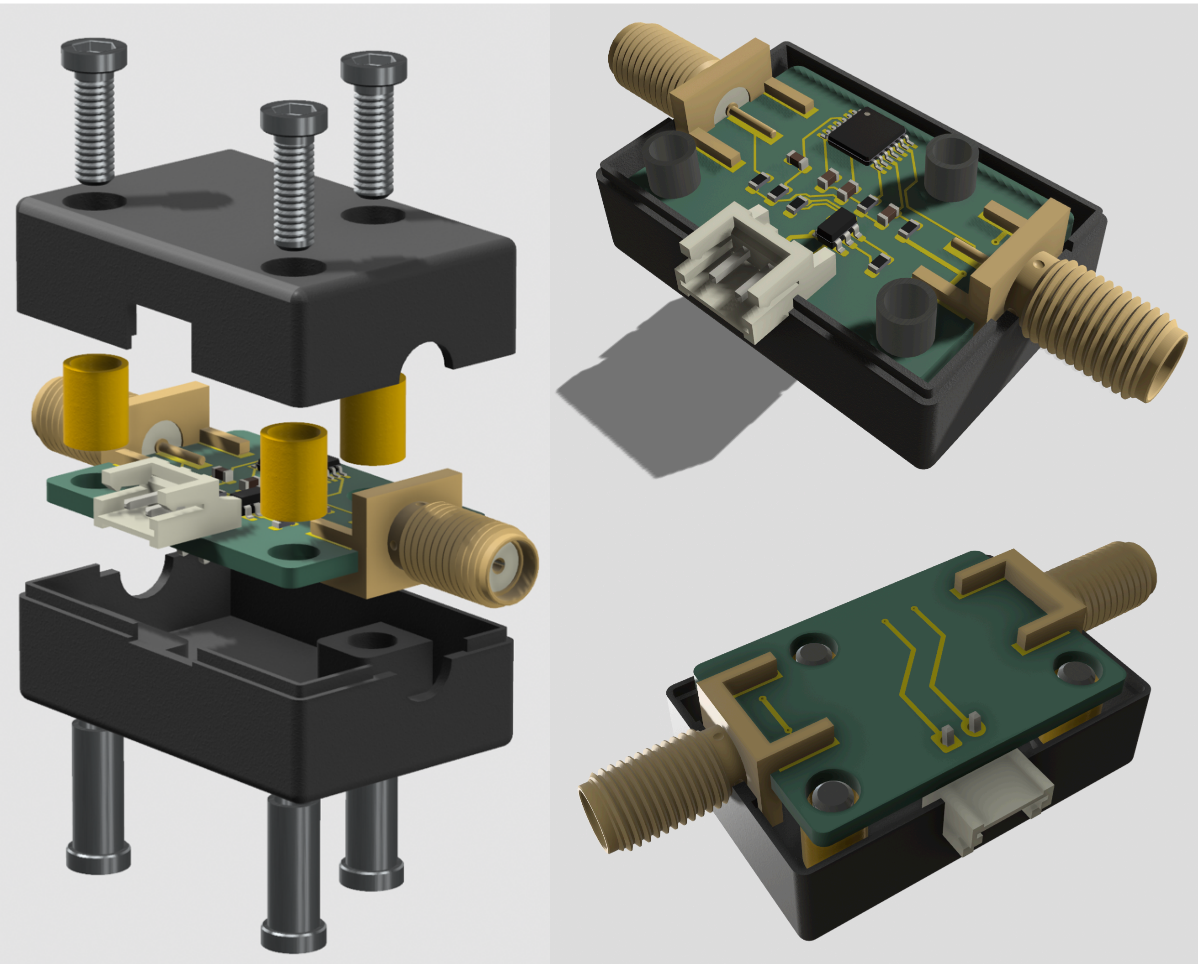

**Figure 14 – 3D model of the entire device in exploded view, with top panel removed, with bottom panel removed. [3]**

## 7.2 Dimensions of the final device

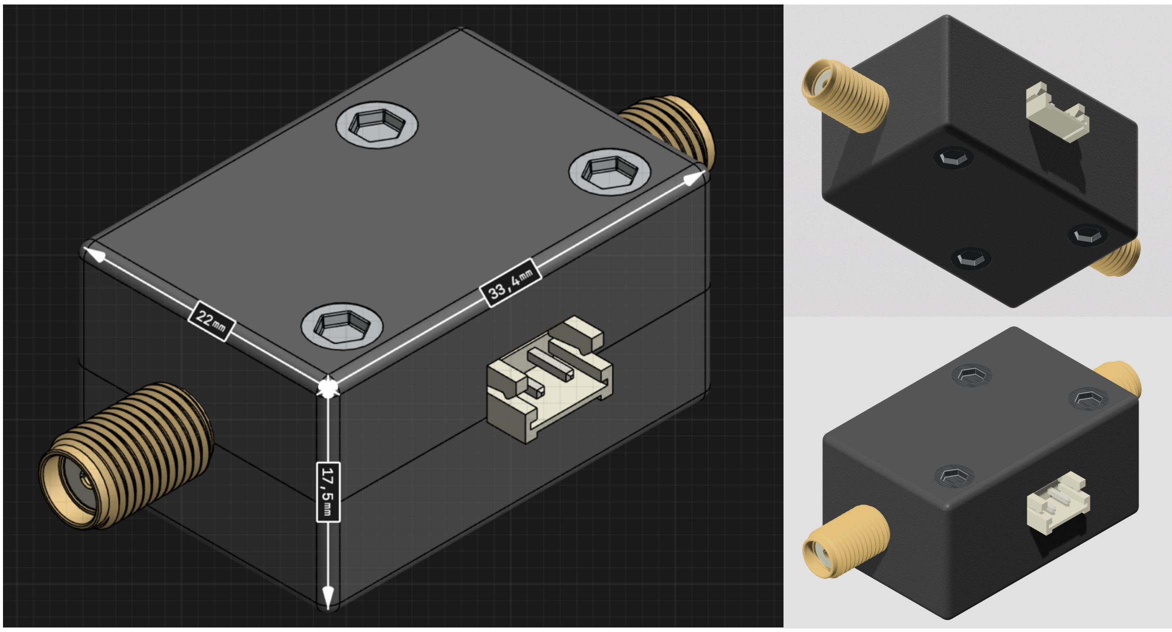


**Figure 15 – 3D model of the device with enclosure measurements & isometric view of the assembled product [3]**

Below, all relevant dimensions of the final, assembled device are listed:

- Dimensions of the PCB:
  $20mm \times 29mm \times 1{,}6mm$
- Dimensions of the PCB with connectors:
  $24{,}5mm \times 51{,}5mm \times 8mm$
- External dimensions of the enclosure:
  $22mm \times 33{,}4mm \times 17{,}5mm$
- dimensions of the device with connectors:
  $25{,}5mm \times 51{,}5mm \times 17{,}5mm$

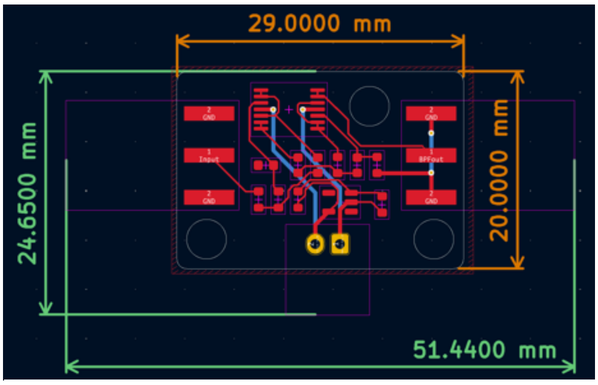


**Figure 16 – PCB dimensions [2]**

Additionally, some dimensions of the device can be seen in figures 15 and 16, alongside the isometric view of the assembled device shown on the left side of figure 15, viewed from bottom and top sides.

## 8. Final product pricing

Table 2 below, shows the full list of all components used for the final product assembly. Each of the components are linked to specific products, with descriptions, prices per unit, units used per device and the product number (when available). The format for the product links is <SellerWebsiteLink>:<ProductNumber>. As "uk.rs-online.com" is commonly used, "RS" is used instead of the full link. All of the prices provided have been gathered based on the **production run of 1000 devices,** hence using bulk discounts were available.

The total price per device, calculated to be approximately **9,445£**, falls between the typical price range observed for commercially available bandpass filters (5£ - 40£). An example of one such device can be seen following the link: https://www.ebay.com/itm/387602688973 . Having said this, similarly priced products mostly showed lower tolerances, use of higher quality components and more complex filter topologies.

**Table 2 – Component list with prices and product numbers, alongside the total price per device**

| Part designator(s) | Component Details | £ per unit | Unit per device | Available / product number |
|---|---|---|---|---|
| PCB | 29mm x 20mm x1.6mm 2-layer FR-4 | 0,045£ | 1 | JLCPCB.com |
| R1, R2, R5, R6 | SMD 26,1kΩ±0.1% 1608 metric resistor | 0,09£ | 4 | RS: 123-9181 |
| R3 | SMD 120kΩ±0.1% 1608 metric resistor | 0,042£ | 1 | RS: 566-373P |
| R4 | SMD 240kΩ±0.1% 1608 metric resistor | 0,077£ | 1 | RS: 168-1005 |
| C1 | SMD 1nF±1% 1608 metric capacitor | 0,018£ | 1 | RS: 169-4089 |
| C2 | SMD 2nF±1% 1608 metric capacitor | 0,027£ | 1 | RS: 146-4336 |
| C3, C4 | SMD 4,7nF±1% 1608 metric capacitor | 0,292£ | 2 | RS: 146-4168 |
| U1 | Quad Op-amp IC MCP6L04T-E/ST | 0,3£ | 1 | RS: 165-3575 |
| U2 | Single Op-amp IC MCP601T-I/OT | 0,394£ | 1 | RS: 628-3475P |
| J1 | JST EH series 2 pin connector | 0,113£ | 1 | RS: 515-1305 |
| J2, J3 | Edge mount SMA coaxial connector | 2,25£ | 2 | RS: 217-7782 |
| Enclosure | 3D printed using PETG material ~10g | 0,149£ | 1 | 3Djake.uk: FF-HDGL-175PNKS-00750 |
| Spacer | 3D printed using PETG material ~0,5g | 0,008£ | 4 | 3Djake.uk: FF-HDGL-175PNKS-00750 |
| Barrel nut | 4mm diameter 12mm length barrel nut | 0,68£ | 4 | Inoxstores.com: 0290620040012 |
| Bolt | 3mm diameter 6mm length bolt | 0,021£ | 4 | Inoxstores.com: 0209120030006 |
| **Total Price Per Device** | **9.445 £** | | | |

Looking at table 2, the most expensive singular component used is the SMA coaxial connector, amounting to 47% of the final device price. For price reduction, an alternative of jack connector can be used (RS: 259-6677, 0,28£) reducing the price to 5,51£. This would require PCB and enclosure modification.

## 9. Product overview and conclusion

The final product was developed to allow for signal filtering using a 2nd order, Sallen-Key bandpass filter. After producing the component values of the filter, the upper and lower cutoff frequencies were shown to equal: $200Hz \pm 1{,}5\% \quad \& \quad 4300Hz \pm 1{,}4\%$, further confirmed using circuit simulations.

The device was designed to be assembled on a custom PCB, using SMD components. Special attention was given to the layout of the PCB to allow for a compact solution. power to the operational amplifiers is supplied via a 5V DC voltage, delivering a minimum power of 3,5mW. A JST connector is used for the power connection, while the input and output signals are interfaced through SMA female connectors.

An enclosure has been designed and modelled using CAD (Computer-aided design) software. The material PETG was chosen to ease the 3D printing of this component. However, a metal enclosure could be considered to improve shielding in electrically noise environments. The 3D model of the final device was rendered to ensure size compatibility of all components.

Overall, the final product successfully meets the design specifications, providing a compact, low-power, low-cost, and accurate bandpass filter solution, suitable for a wide range of signal manipulation applications.

## 10. References

[1] N. Instruments, "Multisim Live," National Instruments, 2024. [Online]. Available: https://www.multisim.com/. [Accessed 17 October 2024].

[2] "KiCad," KiCad Developers, November 2021. [Online]. Available: https://www.kicad.org. [Accessed 20 March 2025].

[3] "Shapr3D CAD software," Shapr3D Inc, 2023. [Online]. Available: https://www.shapr3d.com. [Accessed 20 March 2025].

[4] "Canva Graphic design tool," Canva Pty Ltd, 2023. [Online]. Available: https://www.canva.com. [Accessed 20 March 2025].

[5] "EEE Year 1, Sem2 Labs (project) Instructions," University of Surrey, [Online]. Available: https://surreylearn.surrey.ac.uk/d2l/le/lessons/267955/topics/3239350. [Accessed 23 March 2025].

[6] L. R. &. R. W. schafer, Digital Processing of speech signals, Pearson, 1978.

[7] IPC, "IPC-2221A," May 2003. [Online]. Available: https://www-eng.lbl.gov/~shuman/NEXT/CURRENT_DESIGN/TP/MATERIALS/IPC-2221A(L).pdf. [Accessed 24 April 2025].

[8] Microchip Technology Inc, "MCP6L04 Documentation," 2009. [Online]. Available: https://www.microchip.com/en-us/product/mcp6l04#Documentation. [Accessed 24 April 2025].

**Additional links:**

- Additional information on the operation of Sallen-key topology-based filters: https://trp.org.in/wp-content/uploads/2017/05/AJES-Vol.6-No.1-January-June-2017-pp.23-28.pdf
- Useful links for automated component value calculation:
  LPF: http://www.calculatoredge.com/electronics/sk%20low%20pass.htm
  HPF: https://www.calculatoredge.com/electronics/sk%20high%20pass.htm